

# Functionalized Coronenes: Synthesis, Solid Structure, and Properties

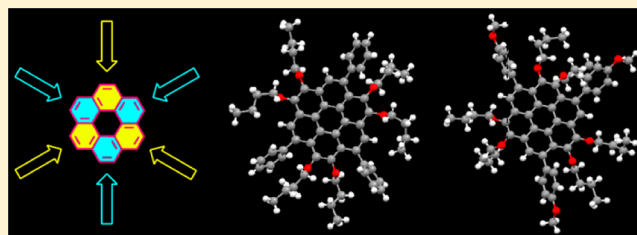
Di Wu,<sup>†</sup> Hua Zhang,<sup>†</sup> Jinhua Liang,<sup>†</sup> Haojie Ge,<sup>†</sup> Chunyan Chi,<sup>‡</sup> Jishan Wu,<sup>‡</sup> Sheng Hua Liu,<sup>\*,†</sup> and Jun Yin<sup>\*,†</sup>

<sup>†</sup>Key Laboratory of Pesticide and Chemical Biology, Ministry of Education, College of Chemistry, Central China Normal University, Wuhan 430079, PR China

<sup>‡</sup>Department of Chemistry, National University of Singapore, 3 Science Drive 3, Singapore 117543, Singapore

## Supporting Information

**ABSTRACT:** The construction of coronenes using simple building blocks is a challenging task. In this work, triphenylene was used as a building block to construct functionalized coronenes, and their solid structures and optoelectronic properties were investigated. The single crystal structures showed that coronenes have different packing motifs. Their good solubility and photostability make them potential solution-processable candidates for organic devices.



Graphene (I) has been widely applied in optoelectronic materials since it was first isolated from graphite by Geim and Novoselov et al. in 2004.<sup>1</sup> Polycyclic aromatic hydrocarbons (PAHs), which make up graphene segments, have large  $\pi$ -conjugated systems and hence are often regarded as promising building blocks for the construction of organic semiconducting materials.<sup>2</sup> Hexa-peri-hexabenzocoronene (HBC, II) is a typical graphene fragment<sup>3</sup> with a  $D_{6h}$ -symmetrical structure and displays outstanding performance in liquid crystal materials due to its strong intermolecular  $\pi$ - $\pi$  interactions and highly ordered columnar packing.<sup>4</sup> Although HBC consists of 13 fused benzene rings, there are more than five strategies to efficiently synthesize functionalized HBCs.<sup>5</sup> Coronene (III) can be regarded as a smaller graphene fragment compared to HBC; it has a unique electronic structure due to the perfect delocalization of the aromaticity among the six outer rings (Scheme 1).<sup>6</sup> In comparison to HBC, coronene as the smallest homologue of benzene with 6-fold symmetry is useful and essential for the film formation and crystallization of molecules.<sup>7</sup> Recently, chemists realized the advantages of smaller  $\pi$ -conjugated coronene and have developed several coronene-based optoelectronic materials.<sup>7,8</sup> Some methods that are based on different building blocks have been developed for the synthesis of coronenes. For example, early synthetic protocols were reported by Newman in 1940,<sup>9</sup> Baker in 1951,<sup>10</sup> Clar in 1957,<sup>11</sup> Craig in 1975,<sup>12</sup> and Reiss in 1977,<sup>13</sup> but they typically suffered from lengthy procedures, low yields, and poor functionalization. In recent years, tremendous efforts have been made to develop new synthetic strategies, including the cyclization of perylene-based dianions,<sup>14</sup> ruthenium-catalyzed benzannulation,<sup>15</sup> Diels–Alder reactions based on perylene-3,4:9,10-bis(dicarboximide)s (PDI) with dienophiles,<sup>8,d,g,16</sup> and the cyclization of 1,7-bis(alkynyl)-substituted PDI.<sup>8a,c,e,17</sup> However, the construction of coronenes using simple starting materials or novel building blocks remains challenging.

As shown in Scheme 1, triphenylene (IV) is one of the segments that can be used to construct coronene. In view of the convenience of its preparation from substituted benzene (V),<sup>18</sup> the use of triphenylene as a building block to construct coronenes offers a convenient and promising approach to advance the functionalization of coronenes. Some reports have indicated that biphenyl acetylenes or phenanthrene-based acetylenes can be cyclized to form aromatic rings in the presence of catalysts such as gold, ruthenium, platinum, and ICl (Scheme 2A).<sup>19</sup> Herein, we used triphenylene as a building block to construct functionalized coronenes with good yields and investigated their solid structures and optoelectronic properties.

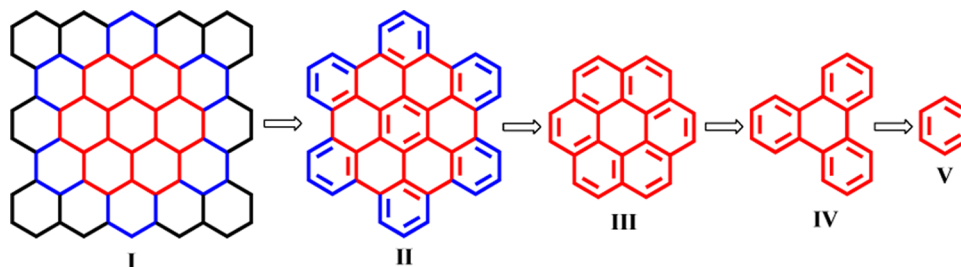
The synthesis of 1a–c is outlined in Scheme 2B. The intermolecular oxidative cyclodehydrogenation reaction of 2 can readily generate 3, which was bromated using bromine to give 4.<sup>20</sup> Subsequently, the palladium-catalyzed Sonogashira coupling reaction was performed to give 5a–c in ~50–54% yields, and 5a–c was subjected to a PtCl<sub>2</sub>-promoted cyclization to afford 1a–c with 52–57% yields. The chemical structures of all new compounds were clearly supported by standard spectroscopic characterizations such as NMR and mass spectrometry (see Supporting Information).

The <sup>1</sup>H NMR spectra of 5a–c revealed three different resonance signals at 9.14–9.48 ppm, indicating that three protons were unsymmetrical. The structures were further identified using X-ray crystallographic analysis. A single crystal of 5a suitable for crystallographic analysis was grown using the diffusion of MeOH to a CH<sub>2</sub>Cl<sub>2</sub> solution of 5a. As depicted in Figure 1A (left), three acetylenyl benzene units were attached on two benzene rings of the triphenylene core. Despite the well-known fact that triphenylene has a completely planar

Received: September 24, 2012

Published: November 27, 2012

Scheme 1. Constructing Fragments of Grapheme



Scheme 2. (A) Cyclization of Acetylenes; (B) Synthesis of Compounds 1a–c

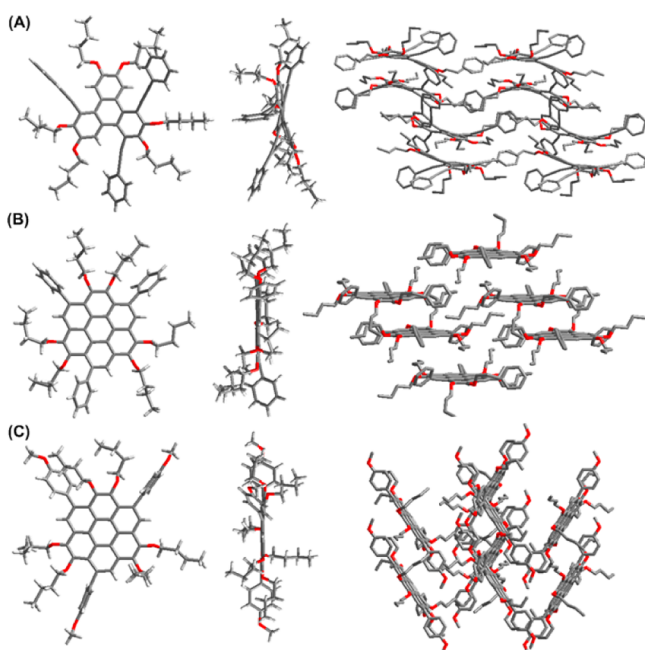
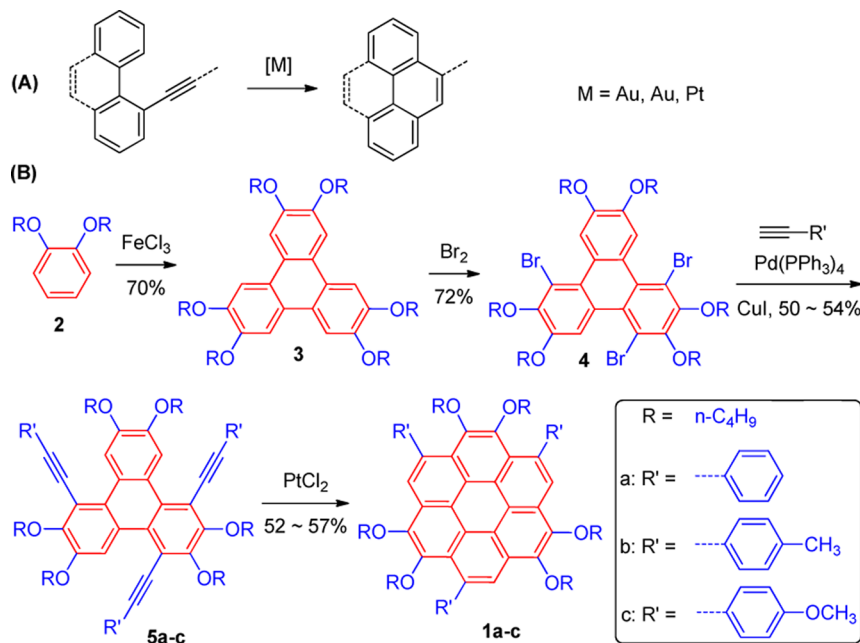


**Figure 1.** Single crystal structures and packing views of **5a** (A), **1a** (B), and **1c** (C). Top, side, and packing view from left to right. Hydrogen atoms have been omitted in packing views.

configuration,<sup>21</sup> the molecule will be twisty when the 1,4,5,8,9,12-positions of triphenylene are substituted, even by small groups such as a methyl group.<sup>22</sup> The single-crystal structure of **5a** displayed a contorted structure in the side view (middle) shown in Figure 1A; this was attributed to the large steric hindrance caused by the substituted groups on the triphenylene. Additionally, the molecules involved in the  $\pi$ - $\pi$  interactions and C-H $\cdots$  $\pi$ , C-H $\cdots$ O hydrogen bonds (see Figure S1 in Supporting Information) led to the ordered packing shown in Figure 1A (right).

In the <sup>1</sup>H NMR spectra for **1a-c**, the resonance of the coronene core displayed 0.15–0.46 ppm upfield shifts compared with the triphenylene core of **5a-c**, and only two peaks could be observed because of the overlapping of the proton signals. Single crystals of **1a** and **1c** suitable for crystallographic analysis were obtained using a method similar to that used for **5a**. As shown in Figure 1B and C, the coronene cores presented an absolutely flat structure. Again, distinct dihedral angles were found between the phenyl moieties and the coronene plane, as a result of the steric effects of the functionalized groups. Both molecules were packed in a one-dimensional columnar structure, and the average distances between the coronene discs were 4.41–4.79 Å.<sup>23</sup> This showed that there were no obvious  $\pi$ - $\pi$  interactions involved in the molecular packing, in contrast with Müllen's report.<sup>7</sup> In that case, weak  $\pi$ - $\pi$  interactions were observed, due to the smaller substituted groups (-OCH<sub>3</sub>). Alter-

natively, the C–H $\cdots\pi$  interaction and C–H $\cdots$ O hydrogen bond promoted ordered packing (Figures S2 and S3 in Supporting Information). Interestingly, two distinct intercolumn packing modes were observed for **1a** and **1c** (Figure 1B and C (right)). **1a** displayed lamellar packing, whereas **1c** formed a herringbone-like packing motif. The slight structural change produced by the introduction of three methoxyl units into **1c** resulted in an obvious change in the packing form. It is well-known that molecular stacking is very important for the properties of a material.<sup>24</sup> Hence, this result afforded an alternative approach to explore organic optoelectronic materials via the simple decoration of their structure. In addition, we used density functional theory (DFT) to optimize their structures at the B3LYP/6-31G\* level in a suite of Gaussian 09 programs. It is worth noting that the results showed good agreement with the crystal structures of **1a** and **1c** (Figures S4 and S6 in Supporting Information). Despite the fact that a single crystal of **1b** was not obtained, it can be easily predicted that **1b** possessed a similar geometry (Figure S5 in Supporting Information). The crystal data and structural refinements of these molecules are summarized, and the bond lengths and angles are listed in the Supporting Information (Tables S1–S6).

Because of the presence of alkoxy chains, these molecules showed very good solubility in common solvents. This good solubility allowed them to be processed in solution and allowed the formation of thin films. The optical properties were investigated using UV–vis absorption and fluorescence spectrometry. Figure 2 shows the UV–vis absorption and

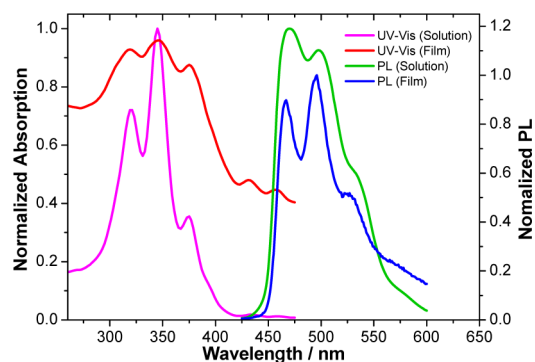


**Figure 2.** Normalized UV–vis absorption and photoluminescence spectra of **1b** in CHCl<sub>3</sub> (1.0 × 10<sup>−5</sup> M) and in thin film.

fluorescence spectra for **1b**. Compared with the *p* band at 342 nm ( $\epsilon = 7.08 \times 10^4 \text{ M}^{-1} \text{ cm}^{-1}$ ) for nonsubstituted coronene,<sup>25</sup> **1b** showed well-resolved absorption bands at 323 and 345 nm,

**Table 1.** Optical and Electrochemical Data of Coronenes **1a–c**

compd	$\lambda_{\text{Abs}}^a$ [nm]	$\lambda_{\text{max}}(\text{PL})^a$ [nm]	$\epsilon_{\text{max}}^b$ [M <sup>−1</sup> cm <sup>−1</sup> ]	$E_{\text{ox}}^1$ [V]	$E_{\text{ox}}^{\text{onset}}$ [V]	HOMO <sup>c</sup> [eV]	LUMO <sup>d</sup> [eV]	$E_g^e$ [eV]	$E_g^f$ [eV]
<b>1a</b>	321, 345, 375 (solution)	470, 498, 534 (solution)	101900	0.84	0.68	−5.48	−2.44	3.07	3.65
	320, 347, 375 (film)	467, 496, 526 (film)							
<b>1b</b>	323, 345, 375 (solution)	472, 498, 536 (solution)	105700	0.88	0.65	−5.45	−2.38	3.07	3.64
	324, 347, 375 (film)	472, 494, 528 (film)							
<b>1c</b>	327, 347, 377 (solution)	474, 501, 540 (solution)	112400	0.78	0.63	−5.43	−2.41	3.02	3.61
	325, 349, 377 (film)	464, 492, 526 (film)							

<sup>a</sup>Wavelength of absorption and photoluminescence in CHCl<sub>3</sub> (1.0 × 10<sup>−5</sup> M). <sup>b</sup>Molar extinction coefficient. <sup>c</sup>HOMO energy levels were calculated from the onset of the first oxidation according to the equation HOMO = −(4.8 +  $E_{\text{ox}}^{\text{onset}}$ ) eV. <sup>d</sup>LUMO = HOMO +  $E_g$ . <sup>e</sup> $E_g$  was calculated from the low-energy absorption onset in the absorption spectra according to the equation  $E_g = 1240/\lambda_{\text{onset}}^{26}$ . <sup>f</sup>Obtained from theoretical calculation by DFT.

with a long-wavelength absorption maximum at 375 nm (*p* band,  $\epsilon_{\text{max}} = 1.06 \times 10^5 \text{ M}^{-1} \text{ cm}^{-1}$ ) in CH<sub>2</sub>Cl<sub>2</sub>, which suggested that the introduction of the three phenyl moieties led to an extended  $\pi$ -conjugation and a red shift of the absorption spectrum.

Similar phenomena were also observed for the absorption spectra of **1a** and **1c** from 300 to 500 nm (Figure S7 in Supporting Information). These results were in agreement with a previous report.<sup>7</sup> Their UV–vis absorption spectra were also measured in the thin-film state. As can be seen in Figure 2 and Table 1, these compounds revealed similar absorption spectra. However, the spectra for the thin films were broader than those measured in solution, indicating that the chromophores had a strong tendency to aggregate in the solid state. We also measured their photoluminescence spectra, which exhibited a 0.95 eV Stokes shift and similar emission (excited at 345 nm, Figure 2). The lower fluorescence quantum yields for **1a–c** (0.098, 0.094, 0.089) could have been due to the symmetric cyclic conjugated structure. It is surprising that **1a–c** possessed very similar optical properties not only in the solution state but also in the thin film state; this indicated that the different substituents (H, Me, and OMe) on the benzene rings had only small effects on their optical properties. The optical energy gaps ( $E_g$ ) of  $\sim 3.02$ – $3.07$  eV were calculated from the low-energy absorption onset in the absorption spectra, as shown in Table 1.

The electrochemical properties of these coronenes were investigated using cyclic voltammetry (CV). The measurements were carried out in dry dichloromethane at room temperature. As shown in Figure 3, two quasi-reversible oxidation waves

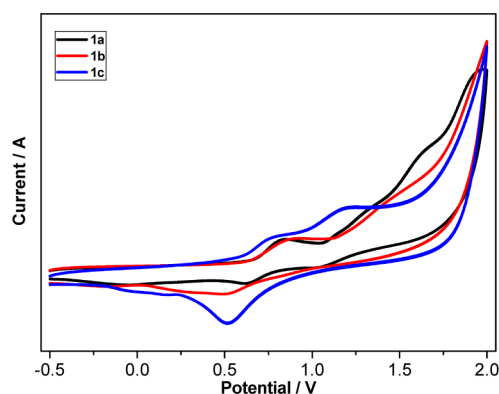


**Figure 3.** Cyclic voltammogram (CV) of coronenes **1a–c** in dry DCM with 0.1 M Bu<sub>4</sub>NPF<sub>6</sub> as supporting electrolyte.

were observed for **1a–c** in the range from 0.50 to 1.00 V. Again, the changes in the substituted groups on the benzene

rings had little effect on the redox behavior of the coronenes **1a–c** (also see data in Table 1). For example, compound **1c** showed two quasi-reversible oxidation waves at 0.78 and 1.21 V (vs Fc/Fc<sup>+</sup>). However, no obvious reduction waves were observed upon a cathodic scan down to  $-2.0$  V. HOMO energy levels of  $-5.48$ ,  $-5.45$ , and  $5.43$  eV were estimated for **1a–c**, respectively, based on the onset potential ( $E_{\text{ox}}^1$ ) of the first oxidation waves. The LUMO energy levels of **1a–c** were calculated on the basis of the equation described in Table 1.<sup>26</sup> From these calculated LUMO levels, we determined that the compounds **1a–c** had similar HOMO and LUMO energy levels because of the small contribution of the substituted groups to the frontier orbitals. To gain a better insight into the molecular orbitals of **1a–c**, the structures and frontier molecular orbital profiles of these coronene molecules were optimized by DFT calculations at the B3LYP/6-31G\* level in a suite of Gaussian 09 programs (Figure S4–S6 in Supporting Information). Figure 4 presents the frontier molecular orbital

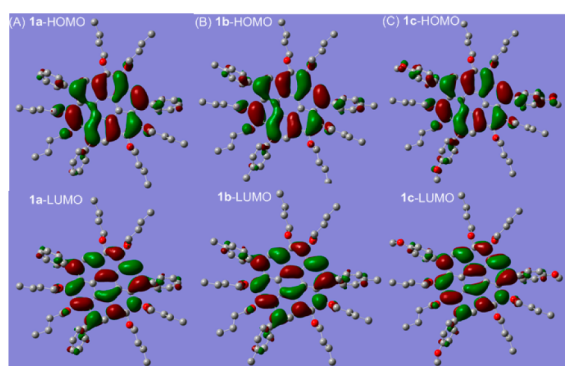


**Figure 4.** Frontier molecular orbital profiles of molecules based on DFT (B3LYP/6-31G\*) calculations.

profiles, which showed that the substituted groups on the benzene rings of coronenes had only slight effects on the molecular orbital profiles. In addition, although the calculated energy gaps (3.65, 3.64, and 3.61 eV) were approximately 0.6 eV higher than the experimental data, the differences between the values for the molecules were negligible, which was in agreement with the experimental data.

The photostability of compounds **1a–c** was investigated in toluene under different irradiation conditions (Figure S8 in Supporting Information). The photoinduced degradation was quantified by monitoring the decrease of absorption in the UV–vis region (325–375 nm). No degradation was observed when compounds **1a–c** were subjected to irradiation with white light (100 W) for 8 h. Furthermore, these compounds revealed only slight decomposition upon irradiation with UV light (6 W) for 8 h. Such remarkable photostability can be ascribed to the high HOMO energy level derived from the coronene core.

In conclusion, three functionalized coronenes were synthesized from triphenylene blocks, with good yields. All of them displayed good solubility and photostability, which makes them potential solution-processable candidates for organic devices. It should be noted that compounds **1a** and **1c** had very different packing motifs in their single crystal structures; this affords an alternative approach to the exploration of organic optoelectronic materials with good performance in devices, using only small amounts of structural decoration. Additionally, it is

worthy of note that successful multiple cyclization can be used to build novel organic conjugated molecules.

## EXPERIMENTAL SECTION

**General Methods.** All manipulations were carried out under an argon atmosphere by using standard Schlenk techniques, unless otherwise stated. All commercials were used as received without further purification. <sup>1</sup>H and <sup>13</sup>C NMR spectra were collected on a 400 or 600 MHz spectrometer. UV–vis and fluorescence spectra were obtained on a UV or fluorescent spectrophotometer, respectively. Mass spectra were measured in the MALDI-TOF mode. The crystal structure was recorded by X-ray diffraction spectrometer. Cyclic voltammetry (CV) was performed on a potentiostat. Elemental analyses were performed by investigation of C, H, N. A three-electrode one-compartment cell was used to contain the solution of complexes and supporting electrolyte in dry CH<sub>2</sub>Cl<sub>2</sub>. Deaeration of the solution was achieved by bubbling argon through the solution for about 10 min before measurement. The ligand and electrolyte (*n*-Bu<sub>4</sub>NPF<sub>6</sub>) concentrations were typically 0.001 and 0.1 M, respectively. A 500 μm diameter platinum disk working electrode, a platinum wire counter electrode, and an Ag/Ag<sup>+</sup> reference electrode were used. The Ag/Ag<sup>+</sup> reference electrode contained an internal solution of 0.01 M AgNO<sub>3</sub> in acetonitrile and was incorporated into the cell with a salt bridge containing 0.1 M *n*-Bu<sub>4</sub>NPF<sub>6</sub> in CH<sub>2</sub>Cl<sub>2</sub>. All electrochemical experiments were carried out under ambient conditions. The theoretical calculation in the present studies were performed at the B3LYP/6-31G\* level by using the Gaussian 03 program.

**General Synthetic Procedure for 5a–c.** A suspension of 1,4,8-tribromo-2,3,6,7,10,11-hexabutoxytriphenylene (2.0 mmol), Pd(PPh<sub>3</sub>)<sub>4</sub> (0.1 mmol), and CuI (0.08 mmol) in a mixture of THF and Et<sub>3</sub>N (50 mL each) was degassed with nitrogen for 15 min at room temperature. Phenylacetylene (6.0 mmol) in THF (50 mL) that was degassed with nitrogen was added to the mixture dropwise with stirring. The mixture was stirred at reflux for 12 h, and then the versatile solvents were removed under reduced pressure. The residue was purified by column chromatography packed with silica gel using dichloromethane/petroleum ether (1:3, v/v) as eluent to afford pure product as a yellow solid.

**Compound 5a.** Yellow solid. Yield: 0.98 g, 51%. Mp = 82–83 °C. <sup>1</sup>H NMR (600 MHz, CDCl<sub>3</sub>): δ 9.44 (s, 1H); 9.21 (s, 1H); 9.15 (s, 1H); 7.56–7.59 (b, 6H, coverlay); 7.35–7.37 (b, 9H, coverlay); 4.23–4.27 (m, 6H); 3.99–4.03 (m, 6H); 1.89–1.91 (m, 6H); 1.64–1.67 (m, 6H); 1.57–1.62 (m, 6H); 1.24–1.27 (m, 6H); 0.96–0.98 (m, 9H); 0.78–0.80 (m, 9H). <sup>13</sup>C NMR (100 MHz, CDCl<sub>3</sub>): δ 153.4, 153.1, 151.6, 149.6, 147.6, 147.3, 132.8, 131.2, 130.0, 128.5, 128.2, 128.0, 127.6, 127.4, 126.2, 125.7, 124.3, 124.0, 123.8, 123.3, 113.7, 113.2, 112.9, 111.7, 110.1, 99.6, 99.0, 98.0, 87.8, 87.6, 73.8, 73.2, 68.5, 68.4, 32.4, 31.0, 26.3, 19.3, 18.8, 13.8, 13.5. MS (MALDI-TOF) *m/z*: calcd for C<sub>66</sub>H<sub>72</sub>O<sub>6</sub> 960.5329, found 960.5371. Anal. Calcd for C<sub>66</sub>H<sub>72</sub>O<sub>6</sub>: C, 82.46; H, 7.55. Found: C, 82.39; H, 7.61.

**Compound 5b.** Yellow solid. Yield: 1.06 g, 53%. Mp = 82–83 °C. <sup>1</sup>H NMR (600 MHz, CDCl<sub>3</sub>): δ 9.44 (s, 1H); 9.23 (s, 1H); 9.16 (s, 1H); 7.44–7.49 (m, 6H); 7.15–7.18 (m, 6H); 4.22–4.26 (m, 6H); 3.99–4.04 (m, 6H); 2.38 (s, 9H); 1.87–1.91 (m, 6H); 1.65–1.71 (m, 6H); 1.59–1.61 (m, 6H); 1.24–1.25 (m, 6H); 0.97–0.98 (m, 9H); 0.80–0.83 (m, 9H). <sup>13</sup>C NMR (100 MHz, CDCl<sub>3</sub>): δ 153.4, 153.2, 149.7, 147.8, 147.4, 138.5, 138.4, 138.1, 131.4, 131.3, 130.0, 129.1, 129.1, 129.0, 128.6, 126.3, 124.5, 124.2, 121.0, 120.6, 113.4, 99.8, 99.3, 98.3, 87.2, 87.2, 87.1, 76.6, 73.9, 73.3, 68.8, 32.5, 31.3, 31.2, 21.4, 19.4, 19.0, 18.9, 13.8, 13.7, 13.6. MS (MALDI-TOF) *m/z*: calcd for C<sub>69</sub>H<sub>78</sub>O<sub>6</sub> 1002.5798, found 1002.5812. Anal. Calcd for C<sub>69</sub>H<sub>78</sub>O<sub>6</sub>: C, 82.60; H, 7.84. Found: C, 82.66; H, 7.79.

**Compound 5c.** Yellow solid. Yield: 1.13 g, 54%. Mp = 82–85 °C. <sup>1</sup>H NMR (400 MHz, CDCl<sub>3</sub>): δ 9.48 (s, 1H); 9.27 (s, 1H); 9.20 (s, 1H); 7.50–7.55 (m, 6H); 6.89–6.92 (m, 6H); 4.23–4.28 (m, 6H); 4.01–4.04 (m, 6H); 3.84 (s, 9H); 1.89–1.91 (m, 6H); 1.71–1.90 (m, 6H); 1.62–1.69 (m, 6H); 1.29–1.31 (m, 6H); 0.96–1.01 (m, 9H); 0.83–0.86 (m, 9H). <sup>13</sup>C NMR (100 MHz, CDCl<sub>3</sub>): δ 159.8, 159.7, 159.5, 153.2, 149.7, 147.6, 147.3, 132.9, 132.8, 132.8, 129.9, 128.6,

126.4, 124.5, 124.2, 116.3, 115.8, 114.1, 114.0, 113.9, 113.8, 113.4, 99.6, 99.1, 98.0, 86.5, 73.9, 73.3, 68.7, 68.6, 55.3, 32.6, 31.3, 31.2, 19.4, 19.0, 18.9, 13.9, 13.7, 13.7. MS (MALDI-TOF)  $m/z$ : calcd for  $C_{69}H_{78}O_9$ , 1050.5646, found 1050.5709. Anal. Calcd for  $C_{69}H_{78}O_9$ : C, 78.83; H, 7.48. Found: C, 78.92; H, 7.56.

**General Synthetic Procedure for 1a–c.** 1,4,8-Triphenyl-2,3,6,7,10,11-hexabutoxytriphenylene (1.0 mmol) was dissolved in 10 mL of dry toluene. After addition of  $PtCl_2$  (0.2 mmol), the reaction vessel was flushed with nitrogen and stirred at 90 °C for 48 h. The solvent was removed under reduced pressure. The residue was purified by column chromatography packed with silica gel using dichloromethane/petroleum ether (1:4, v/v) as eluent to afford pure product as an orange solid.

**Compound 1a.** Orange solid. Yield: 0.51 g, 51%. Mp = 143–145 °C.  $^1H$  NMR (400 MHz,  $CDCl_3$ ):  $\delta$  9.01–9.03 (s, 3H, coverlay); 7.78–7.80 (b, 6H, coverlay); 7.49–7.54 (b, 9H, coverlay); 4.55 (b, 6H, coverlay); 3.79 (b, 6H, coverlay); 2.00–2.05 (m, 6H); 1.69–1.70 (m, 6H); 1.03–1.11 (m, 9H), 0.79–0.85 (m, 9H).  $^{13}C$  NMR (100 MHz,  $CDCl_3$ ):  $\delta$  146.4, 146.0, 145.5, 144.5, 144.4, 137.0, 136.8, 136.5, 129.8, 129.7, 129.6, 127.0, 126.9, 126.1, 124.5, 124.4, 124.4, 124.2, 124.0, 123.1, 122.8, 122.6, 121.7, 121.4, 120.1, 119.8, 74.2, 74.1, 73.7, 73.7, 32.8, 32.7, 32.6, 31.1, 31.0, 19.6, 19.5, 19.1, 19.0, 14.0. MS (MALDI-TOF)  $m/z$ : calcd for  $C_{66}H_{72}O_6$ , 960.5329, found 960.5375. Anal. Calcd for  $C_{66}H_{72}O_6$ : C, 82.46; H, 7.55. Found: C, 82.31; H, 7.39.

**Compound 1b.** Orange solid. Yield: 0.53 g, 53%. Mp = 120–122 °C.  $^1H$  NMR (400 MHz,  $CDCl_3$ ):  $\delta$  8.99–9.01 (s, 3H, coverlay); 7.79 (b, 6H, coverlay); 7.34–7.36 (m, 6H); 4.53–4.55 (m, 6H); 3.76–3.78 (m, 6H); 2.55 (s, 9H); 2.01–2.03 (m, 6H); 1.66–1.68 (m, 6H); 1.03–1.25 (m, 21H); 0.79–0.85 (m, 9H).  $^{13}C$  NMR (100 MHz,  $CDCl_3$ ):  $\delta$  147.7, 146.5, 146.4, 146.0, 145.8, 144.4, 144.4, 142.7, 137.0, 136.8, 136.5, 135.5, 129.8, 129.7, 129.6, 129.5, 127.7, 127.6, 124.4, 124.2, 124.0, 124.0, 122.9, 122.9, 121.8, 119.7, 74.2, 74.1, 73.7, 73.6, 32.7, 32.6, 31.3, 31.2, 21.3, 19.5, 19.1, 19.0, 14.1, 14.1, 14.1, 14.0. MS (MALDI-TOF)  $m/z$ : calcd for  $C_{69}H_{78}O_6$ , 1002.5798, found 1002.5834. Anal. Calcd for  $C_{69}H_{78}O_6$ : C, 82.60; H, 7.84. Found: C, 82.71; H, 7.96.

**Compound 1c.** Orange solid. Yield: 0.60 g, 57%. Mp = 165–167 °C.  $^1H$  NMR (400 MHz,  $CDCl_3$ ):  $\delta$  8.99–9.01 (s, 3H, coverlay); 7.70–7.74 (m, 6H); 7.08–7.11 (m, 6H); 4.54–4.56 (m, 6H); 3.97 (s, 9H); 3.76–3.78 (m, 6H); 2.03–2.05 (m, 6H); 1.69–1.71 (m, 6H); 1.04–1.26 (m, 21H); 0.79–0.88 (m, 9H).  $^{13}C$  NMR (100 MHz,  $CDCl_3$ ):  $\delta$  158.4, 147.7, 147.6, 146.5, 145.9, 144.4, 144.3, 138.0, 138.0, 136.4, 136.1, 130.8, 130.7, 130.7, 124.5, 124.3, 124.2, 124.0, 123.0, 122.8, 122.6, 122.3, 121.8, 121.5, 120.0, 119.8, 119.4, 112.6, 112.4, 74.2, 74.1, 73.8, 55.4, 32.7, 32.6, 31.3, 30.9, 19.5, 19.1, 19.0, 14.1. MS (MALDI-TOF)  $m/z$ : calcd for  $C_{69}H_{78}O_9$ , 1050.5646, found 1050.5680. Anal. Calcd for  $C_{69}H_{78}O_9$ : C, 78.83; H, 7.48. Found: C, 78.66; H, 7.33.

## ■ ASSOCIATED CONTENT

### Supporting Information

Details on the synthesis, characterization, NMR, MS spectra of interminates and coronenes. This material is available free of charge via the Internet at <http://pubs.acs.org>.

## ■ AUTHOR INFORMATION

### Corresponding Author

\*E-mail: yinj@mail.ccnu.edu.cn; chshliu@mail.ccnu.edu.cn.

### Notes

The authors declare no competing financial interest.

## ■ ACKNOWLEDGMENTS

This work was financially supported by National Natural Science Foundation of China (Nos. 20931006, 21072070, 21072071), Program for Changjiang Scholars and Innovative Research Team in University (No. IRT0953), the Program for Academic Leader in Wuhan Municipality (No.201271130441), and self-determined research funds of CCNU from the college's basic research and operation of MOE. We thank Dr. Xianggao

Meng for measurement and analysis of single crystal structures and Dr. Yanliang Ren for theoretical calculation. We thank Prof. Anxin Wu for his suggestions and dedicate to him on the occasion of his 50th birthday.

## ■ REFERENCES

- (1) Novoselov, K. S.; Geim, A. K.; Morozov, S. V.; Jiang, D.; Zhang, Y.; Dubonos, S. V.; Grigorieva, I. V.; Firsov, A. A. *Science* **2004**, *306*, 666.
- (2) For selected reviews, see: (a) Wu, J. *Curr. Org. Chem.* **2007**, *11*, 1220. (b) Pisula, W.; Feng, X.; Müllen, K. *Chem. Mater.* **2011**, *23*, 554. (c) Meng, Q.; Dong, H.; Hu, W.; Zhu, D. *J. Mater. Chem.* **2011**, *21*, 11708.
- (3) Hill, J. P.; Jin, W.; Kosaka, A.; Fukushima, T.; Ichihara, H.; Shimomura, T.; Ito, K.; Hashizume, T.; Ishii, N.; Aida, T. *Science* **2004**, *304*, 1481.
- (4) For selected reviews, see: (a) Simpson, C. D.; Wu, J.; Watson, M. D.; Müllen, K. *J. Mater. Chem.* **2004**, *14*, 494. (b) Grimsdale, A. C.; Wu, J.; Müllen, K. *Chem. Commun.* **2005**, 2197. (c) Sergeyev, S.; Pisula, W.; Geerts, Y. H. *Chem. Soc. Rev.* **2007**, *36*, 1902. (d) Pisula, W.; Feng, X.; Müllen, K. *Adv. Mater.* **2010**, *22*, 3634.
- (5) Wu, J.; Pisula, W.; Müllen, K. *Chem. Rev.* **2007**, *107*, 718.
- (6) Fetzer, J. C. *The Chemistry and Analysis of the Large Polycyclic Aromatic Hydrocarbons*; Wiley: New York, 2000.
- (7) Rieger, R.; Kastler, M.; Enkelmann, V.; Müllen, K. *Chem.—Eur. J.* **2008**, *14*, 6322.
- (8) (a) Rohr, U.; Schlichting, P.; Böhm, A.; Gross, M.; Meerholz, K.; Bräuchle, C.; Müllen, K. *Angew. Chem.* **1998**, *110*, 1463. (b) Chi, X.; Besnard, C.; Thorsmølle, V. K.; Butko, V. Y.; Taylor, A. J.; Siegrist, T.; Ramirez, A. P. *Chem. Mater.* **2004**, *16*, 5751. (c) Nolde, F.; Pisula, W.; Müller, S.; Kohl, C.; Müller, K. *Chem. Mater.* **2006**, *18*, 3715. (d) Alibert-Fouet, S.; Seguy, I.; Bobo, J. -F.; Destruel, P.; Bock, H. *Chem.—Eur. J.* **2007**, *13*, 1746. (e) An, Z.; Yu, J.; Domercq, B.; Jones, S. C.; Barlow, S.; Kippelen, B.; Marder, S. R. *J. Mater. Chem.* **2009**, *19*, 6688. (f) Jia, H. P.; Liu, S. X.; Sanguinet, L.; Levillain, E.; Decurtins, S. *J. Org. Chem.* **2009**, *74*, 5727. (g) Ghosh, A.; Rao, K. V.; George, S. J.; Rao, C. N. R. *Chem.—Eur. J.* **2010**, *16*, 2700.
- (9) Newma, M. S. *J. Am. Chem. Soc.* **1940**, *62*, 1683.
- (10) Baker, W.; Glockling, F.; Mcomie, J. F. W. *J. Chem. Soc.* **1951**, 1118.
- (11) Clar, E.; Zander, M. *J. Chem. Soc.* **1957**, 4616.
- (12) Craig, J. T.; Halton, B.; Lo, S.-F. *Aust. J. Chem.* **1975**, *28*, 913.
- (13) Jessup, P. J.; Reiss, J. A. *Aust. J. Chem.* **1977**, *30*, 843.
- (14) Dijk, J. T. M.; Van, Hartwijk, A.; Bleeker, A. C.; Lugtenburg, J.; Cornelisse, J. *J. Org. Chem.* **1996**, *61*, 1136.
- (15) Shen, H. -C.; Tang, J. -M.; Chang, H. -K.; Yang, C. -W.; Liu, R. -S. *J. Org. Chem.* **2005**, *70*, 10113.
- (16) (a) Langhals, H.; Grundner, S. *Chem. Ber.* **1986**, *119*, 2373. (b) Yang, B.; Li, Y.; Xie, M. G. *Chin. Chem. Lett.* **2003**, *14*, 783. (c) Rao, K. V.; George, S. J. *Org. Lett.* **2010**, *12*, 2656.
- (17) (a) Franceschin, M.; Alvino, A.; Ortaggi, G.; Bianco, A. *Tetrahedron Lett.* **2004**, *45*, 9015. (b) Franceschin, M.; Alvino, A.; Casagrande, V.; Mauriello, C.; Pascucci, E.; Savino, M.; Ortaggi, G.; Bianco, A. *Bioorg. Med. Chem.* **2007**, *15*, 1848. (c) Lee, I. H.; Jeon, Y. M.; Gong, M. -S. *Synth. Met.* **2008**, *158*, 532. (d) Yan, Q.; Cai, K.; Zhang, C.; Zhao, D. *Org. Lett.* **2012**, *14*, 4654.
- (18) Pérez, D.; Guitián, E. *Chem. Soc. Rev.* **2004**, *33*, 274.
- (19) (a) Mamane, V.; Hannen, P.; Fürstner, A. *Chem.—Eur. J.* **2004**, *10*, 4556. (b) Storch, J.; Čermák, J.; Karban, J. *Tetrahedron Lett.* **2007**, *48*, 6814. (c) Xie, C.; Zhang, Y.; Yang, Y. *Chem. Commun.* **2008**, 4810. (d) Chen, T.-A.; Lee, T.-J.; Lin, M.-Y.; Sohel, S. M. A.; Diau, E. W.-G.; Lush, S.-F.; Liu, R.-S. *Chem.—Eur. J.* **2010**, *16*, 1826. (e) Walker, D. B.; Howgego, J.; Davis, A. O. *Synthesis* **2010**, 3686. (f) Matsuda, T.; Moriya, T.; Goya, T.; Murakami, M. *Chem. Lett.* **2011**, *40*, 40. (g) Shaibu, B. S.; Lin, S.-H.; Lin, C.-Y.; Wong, K.-T.; Liu, R.-S. *J. Org. Chem.* **2011**, *76*, 1054. (h) Yao, T.; Campo, M. A.; Larock, R. C. *Org. Lett.* **2004**, *6*, 2677. (i) Yao, T.; Campo, M. A.; Larock, R. C. *J. Org. Chem.* **2005**, *70*, 3511. (j) Li, C.-W.; Wang, C.-I.; Liao, H.-Y.;

Chaudhuri, R.; Liu, R.-S. *J. Org. Chem.* **2007**, *72*, 9203. (k) Mukherjee, A.; Pati, K.; Liu, R.-S. *J. Org. Chem.* **2009**, *74*, 6311.

(20) Li, Z.; Zhi, L.; Lucas, N. T.; Wang, Z. *Tetrahedron* **2009**, *65*, 3417.

(21) (a) Andresen, T. L.; Krebs, F. C.; Thorup, N.; Bechgaard, K. *Chem. Mater.* **2000**, *12*, 2428. (b) Zyss, J.; Ledoux-Rak, I.; Weiss, H.-C.; Bläser, D.; Boese, R.; Thallapally, P. K.; Thalladi, V. R.; Desiraju, G. R. *Chem. Mater.* **2003**, *15*, 3063.

(22) Wang, Y.; Stretton, A. D.; McConnell, M. C.; Wood, P. A.; Parsons, S.; Henry, J. B.; Mount, A. R.; Galow, T. H. *J. Am. Chem. Soc.* **2007**, *129*, 13193.

(23) Tauer, T. P.; Derrick, M. E.; Sherrill, C. D. *J. Phys. Chem. A.* **2005**, *109*, 191.

(24) Jiang, L.; Dong, H.; Hu, W. *J. Mater. Chem.* **2010**, *20*, 4994.

(25) Scholl, R.; Meyer, K. *Ber. Dtsch. Chem. Ges.* **1932**, *65*, 902.

(26) Chi, C.; Wegner, G. *Macromol. Rapid Commun.* **2005**, *26*, 1532.